Molecules and Cells

Biochemical Characterization of the Num1-Mdm36 Complex at the Mitochondria-Plasma Membrane Contact Site

Jongdae Won, Yuri Choi, Yaejin Yun, and Hyung Ho Lee*

Department of Chemistry, College of Natural Sciences, Seoul National University, Seoul 08826, Korea
*Correspondence: hyungholee@snu.ac.kr
https://doi.org/10.14348/molcells.2021.0016
www.molcells.org

In eukaryotic cells, organelles are distributed and positioned in proximity to each other through molecular tether proteins. Among these, the mitochondria-endoplasmic reticulum cortex anchor (MECA) is a well-known tethering complex in *Saccharomyces cerevisiae* that tethers mitochondria to the plasma membrane and plays a key role in mitochondrial fission. The main components of MECA are Num1 and Mdm36, and it is known that Mdm36 binds to Num1 to enhance mitochondrial tethering. To better understand the biochemical characteristics of the Num1-Mdm36 complex at the molecular level, we purified the coiled-coil domain of Num1, full-length Mdm36, and Num1-Mdm36 complex and identified the oligomeric state and stoichiometric characteristics of the Num1-Mdm36 complex by chemical crosslinking, size-exclusion chromatography coupled with multi-angle light scattering, and isothermal titration calorimetry. Mdm36 exists as a dimer and interacts preferentially with Num1 with a stoichiometry of 2:2, forming a heterotetrameric complex. Furthermore, we narrowed down the specific binding region of Num1, which is essential for interacting with Mdm36, and showed that their binding affinity is strong enough to tether both mitochondrial and plasma membranes. Our biochemical characterizations suggest a stoichiometric model of the Num1-Mdm36 complex at the mitochondria-plasma membrane contact site in budding yeast.

Keywords: Mdm36, mitochondria, Num1, plasma membrane, tethering

INTRODUCTION

Although eukaryotic subcellular organelles are compartmented, they continuously communicate with each other across membranes through various mechanisms, such as diffusion or active transport, and vesicular trafficking (Prinz et al., 2020). In addition, one of the ubiquitous and widespread communication strategies between organelles is through close contact (Shai et al., 2018; Valm et al., 2017). These contact regions between heterologous membranes are defined as membrane contact sites (MCSs) (Eisenberg-Bord et al., 2016; Helle et al., 2013). These MCSs enable inter-organelle communication by distributing and positioning organelles in proximity through molecular tether proteins.

There are various MCSs in cells and each has distinct functions (Helle et al., 2013). For example, the endoplasmic reticulum (ER)-mitochondria MCS (de Brito and Scorrano, 2008; Rizzuto et al., 1998) is crucial for the exchange of calcium ions (Rizzuto et al., 1998), transfer of phospholipids in a non-vesicular manner, and reactive oxygen species signaling (Booth et al., 2016; Hayashi et al., 2009; Naon and Scorrano, 2014). The ER-plasma membrane MCS is related to autophagosome biogenesis (Nascimbeni et al., 2017)

Received 23 January, 2021; revised 3 March, 2021; accepted 3 March, 2021; published online 8 April, 2021

eISSN: 0219-1032

and the mitochondria-Golgi MCS to apoptosis (Ouasti et al., 2007). There are many more combinations of organelles forming MCSs that were recently discovered, such as mitochondria-dark-vacuole bodies (Dong et al., 2020), peroxisome-plasma membranes, and lipid droplet-vacuoles (Huang et al., 2020; Kakimoto et al., 2018).

Plasma membrane-mitochondrial MCS and their associated tethering proteins have been better studied in yeast. The mitochondria-ER cortex anchor (MECA) is one of the tethers involved in proper mitochondrial positioning along with Mmr1 and Mfb1 (Kraft and Lackner, 2018). Unlike Mmr1, which is proposed to anchor mitochondria at the bud tip (Chen et al., 2018), MECA tethers mitochondria to the plasma membrane in the mother cell, which is important for mitochondrial fission and partitioning (Lackner et al., 2013). The two main components of MECA in budding yeast are Num1 and Mdm36. Num1 is a 313 kDa protein that was first identified through its function in nuclear migration (Kormanec et al., 1991). It contains an N-terminal coiled-coil domain and C-terminal pleckstrin homology (PH) domain, and each domain is associated with an interaction with the mitochondria and plasma membrane, respectively, with different lipid-binding specificities (Ping et al., 2016). An asymmetric mitochondrial distribution towards the bud was observed in mutants lacking Num1, suggesting that Num1 plays a role in retaining mitochondria in the mother cell (Cerveny et al., 2007).

Moreover, it is known that Mdm36, which is peripherally bound to the mitochondrial surface and acts as a fission promoter (Hammermeister et al., 2010; Westermann, 2015), interacts with Num1 and facilitates proper localization of Num1 in mitochondria (Lackner et al., 2013). This is supported by the result that the loss of mitochondrial cell cortex attachment in Mdm36 deletion mutants resulted in mitochondrial fission defects (Hammermeister et al., 2010). Furthermore, a yeast mutant with deletions in both Num1 and Mdm36 resulted in a strong reduction in the mitochondrial fission machinery (Cerveny et al., 2007; Hammermeister et al., 2010; Lackner et al., 2013). Taken together, both Num1 and Mdm36 are required for proper mitochondrial tethering to the plasma membrane in budding yeast. However, the structural and biochemical details, such as stoichiometry and binding affinity between Num1 and Mdm36 remain elusive. These details are essential for a better understanding of the molecular mechanism of tethering in mitochondrial fission.

In this study, we purified the coiled-coil domain of Num1 (hereafter referred to as Num1CC), full-length Mdm36, and the Num1CC-Mdm36 complex, and identified the oligomeric state and stoichiometric characteristics of the Num1CC-Mdm36 complex by performing experiments, such as chemical crosslinking, size-exclusion chromatography coupled with multi-angle light scattering (SEC-MALS), and isothermal titration calorimetry (ITC). Mdm36 exists as a dimer and interacts preferentially with Num1CC with a stoichiometry of 2:2, forming a heterotetrameric complex. Furthermore, we narrowed down the specific binding region of Num1CC required for interaction with Mdm36. Based on our results, we suggest a more comprehensive architecture of the Num1-Mdm36 complex at the mitochondria-plasma MCS.

MATERIALS AND METHODS

Cloning, expression, and purification of Num1 and Mdm36

The DNA of the coiled-coil domain of Num1 comprising residues 97-294 and full-length Mdm36 comprising residues 1-579 were polymerase chain reaction-amplified from cDNA of *Saccharomyces cerevisiae* and separately subcloned into pGST2 vectors in frame with an N-terminal GST tag and TEV protease recognition site. Num1CC was expressed and purified as follows: Num1CC was expressed in *Escherichia coli* Rosetta II pLysS (Invitrogen, USA). Cells were grown in LB broth supplemented with 100 μg/ml ampicillin and 35 μg/ml chloramphenicol at 37°C, induced with 0.5 mM isopropyl-β-D-1-thiogalactopyranoside (IPTG) when the optical density at 600 nm (OD_{600}) reached 0.6-1.0, and further incubated at 18°C for 16 h. Cells were harvested and stored at −80°C until use. Cells were resuspended in ice-cold lysis buffer (20 mM Tris-HCl pH 8.0, and 200 mM NaCl) supplemented with 1 mM phenylmethylsulphonyl fluoride (PMSF). Cells were disrupted with a microfluidizer (Microfluidics, USA) and centrifuged at 20,000*g* at 4°C for 30 min to remove cell debris. The supernatant was applied to Glutathione Sepharose 4 B resin (Cytiva, USA) pre-equilibrated with lysis buffer. The resin was washed with 20 column volumes of lysis buffer, and Num1CC was eluted with a solution containing 50 mM reduced glutathione. The elutes were buffer-exchanged into buffer A (20 mM Tris-HCl pH 8.0, 50 mM NaCl, and 5 mM β-mercaptoethanol), and the N-terminal GST tag was cleaved by TEV protease overnight at 4°C. GST-cleaved Num1CC was further purified by cation-exchange chromatography using a HiTrap SP-HP column (Cytiva). The proteins were bound to the resin by passing through the column, and the bound proteins were eluted with gradient buffer A into buffer B (20 mM Tris-HCl pH 8.0, 1 M NaCl, and 5 mM β-mercaptoethanol). Final purification was performed by size-exclusion chromatography on a HiLoad 16/60 Superdex 200 prep-grade column (Cytiva), which was equilibrated with buffer C (20 mM Tris-HCl pH 8.0, 200 mM NaCl).

Mdm36 was expressed and purified as previously described for Num1CCs with the following modifications. Mdm36 was expressed in *E. coli* Rosetta II (Invitrogen). Cells were grown in LB broth supplemented with 100 μg/ml ampicillin and 35 μg/ml chloramphenicol at 37°C, induced with 0.2 mM IPTG when the OD_{600} reached 0.6-1.0, and further incubated at 18°C for 16 h. Cells were harvested and stored at −80°C until use. Cells were resuspended in ice-cold lysis buffer supplemented with 1 mM PMSF. Cells were disrupted with a microfluidizer (Microfluidics) and centrifuged at 20,000*g* at 4°C for 30 min to remove cell debris. The supernatant was applied to Glutathione Sepharose 4 B (Cytiva) pre-equilibrated with lysis buffer. The resin was washed with 20 column volumes of lysis buffer, and Mdm36 was eluted with a buffer containing 15 mM reduced glutathione. The elutes were buffer-exchanged into buffer A, and the N-terminal GST tag was cleaved by TEV protease overnight at 4°C. GST-cleaved Mdm36 was further purified by anion-exchange chromatography using a HiTrap Q-HP column (Cytiva). The proteins were bound to the resin by passing through the column, and the bound proteins

were eluted with gradient buffer A into buffer B. Final purification was performed by size-exclusion chromatography on a HiLoad 16/60 Superdex 200 prep-grade column (Cytiva), which was equilibrated with buffer C. The homogeneity of the protein in each purification step was assessed by polyacrylamide gel electrophoresis in the presence of 0.1% (w/v) sodium dodecyl sulfate (SDS-PAGE). For truncated Num1CCs (Num1 [97-195], Num1 [196-294], Num1 [117-195], and Num1 [97-175]), all expression and purification processes were identical to those of Num1CC except that no further purification was performed after GST-affinity chromatography and TEV protease cleavage.

Analytical size-exclusion chromatography

Purified Mdm36 and Num1CC proteins were mixed at a molar ratio of 1:1 and incubated for 1 h at 4°C. After brief centrifugation, 100 μl of the sample was injected into a Superdex 200 10/300 GL column (Cytiva) that was pre-equilibrated with buffer C. A standard curve was obtained using molecular weight markers (Sigma-Aldrich, USA). The Stokes radii of β-amylase, alcohol dehydrogenase, carbonic anhydrase, and cytochrome C were calculated from the crystal structures of each protein (Protein Data Bank [PDB] codes: 1FA2, 2HCY, 1V9E, and 1HRC, respectively) using the *HYDROPRO* program (data not shown) (García De La Torre et al., 2000).

SEC-MALS

SEC-MALS experiments for Num1CC, Mdm36, and the Num1CC-Mdm36 complex were performed using an FPLC system (AKTA Pure; Cytiva) connected to a Wyatt MiniDAWN TREOS MALS instrument and a Wyatt Optilab rEX differential refractometer. A Superdex 200 10/300 GL (Cytiva) size-exclusion chromatography column pre-equilibrated with buffer C, was normalized using ovalbumin. Proteins were injected at a flow rate of 0.4 ml/min. Data were analyzed using the Zimm model for static light-scattering data fitting and graphs were constructed using the EASI graph with a UV peak in the ASTRA VI software (Wyatt, USA).

Isothermal titration calorimetry

ITC experiments were performed using Affinity ITC instruments (TA Instruments, USA) at 298 K. A 100 μM sample of Mdm36 was prepared in buffer C. Buffer and water used in this experiment were degassed at 295 K in advance. Using a micro-syringe, 2.5 μl of 1.5 mM Num1CC was added at intervals of 200 s to the Mdm36 proteins in the cell with gentle stirring.

Chemical crosslinking

The oligomeric states of Num1CC, Mdm36, and their complexes were assessed by chemical cross-linking using an amine-group-specific crosslinker, BS3 (Sulfo-DSS; Thermo Fisher Scientific, USA), according to the manufacturer's protocol. In brief, purified Num1CC and Mdm36 proteins were buffer-exchanged from buffer C to a buffer consisting of 20 mM HEPES, at pH 7.5, and 200 mM NaCl to remove Tris-base in the solution, which may interfere with the crosslinking reaction. BS3 was first dissolved in water to a concentration of 50 mM and further diluted to 5 mM with buffer C. Protein samples (10 μM) were mixed with 500 μM BS3 and incubated at room temperature for 30 min. The reactions were quenched by adding 1.5 M Tris-HCl, pH 7.5, to a final concentration of 50 mM, and the reactants were analyzed by SDS-PAGE after brief centrifugation at 20,000*g* for 10 min to remove aggregation.

RESULTS AND DISCUSSION

In vitro assembly of the Num1-Mdm36 complex

To confirm the interaction between Num1 and Mdm36, we expressed the coiled-coil domain of Num1 (amino acids 97-294; hereafter Num1CC) and Mdm36 (amino acids 1-579) in *E. coli* and purified both proteins separately. Both proteins were fused with the N-terminal GST tag, which was used for GST-affinity purification. After TEV protease addition for GST cleavage and GST removal by ion-exchange chromatography, both proteins were further purified by size-exclusion chromatography (Figs. 1A and 1B). Moreover, the purified Num1CC and Mdm36 samples were analyzed by size-exclusion chromatography coupled with multiangle light scattering (SEC-MALS) to measure their molecular weights in solution. The results revealed that both proteins exist as dimers, which are consistent with previous studies (Ping et al., 2016; Tang et al., 2012) (Fig. 1C). Next, we performed chemical crosslinking using the BS3 crosslinker in the Num1CC, Mdm36, and Num1CC-Mdm36 mixtures. The BS3 crosslinking results showed that Num1CC and Mdm36 exist as dimers, but they also directly interact with each other and form a stable protein complex (Fig. 1D). Interestingly, the newly formed Num1CC-Mdm36 complex band after crosslinking had a higher molecular weight than that of the Mdm36 dimer, which suggests that the dimer form of Mdm36 participates in the direct interaction with Num1CC (Fig. 1D).

Biochemical characterization of the Num1-Mdm36 complex

To identify the oligomeric property of the Num1CC-Mdm36 complex in solution, we purified the Num1CC-Mdm36 complex. Purified Num1CC and Mdm36 proteins were mixed, and fractions comprising the Num1CC-Mdm36 complex were pooled after size-exclusion chromatography (Fig. 2A). Next, we performed SEC-MALS with the purified Num1CC-Mdm36 complex. The SEC-MALS experiment showed that the molecular weight of the Num1CC-Mdm36 complex is 173.8 kDa, which corresponds to the sum of the molecular weight of dimeric Num1CC and dimeric Mdm36. This indicated that the Num1CC-Mdm36 complex exists as a hetero-tetramer in solution, considering the molecular weight of monomeric Num1CC (24 kDa) and monomeric Mdm36 (67 kDa) (Fig. 2B).

To investigate the binding affinity of Num1CC for Mdm36 and the exact stoichiometry of the Num1CC-Mdm36 complex, we performed ITC. ITC experiments showed that the complex formation reaction was endothermic, and the dissociation constant value (K_D) between Num1CC and Mdm36 was 121 nM (Fig. 2C). The binding affinity between Num1CC and Mdm36 is very similar to other tethering factors, and the affinity might be strong enough not to be fallen apart during

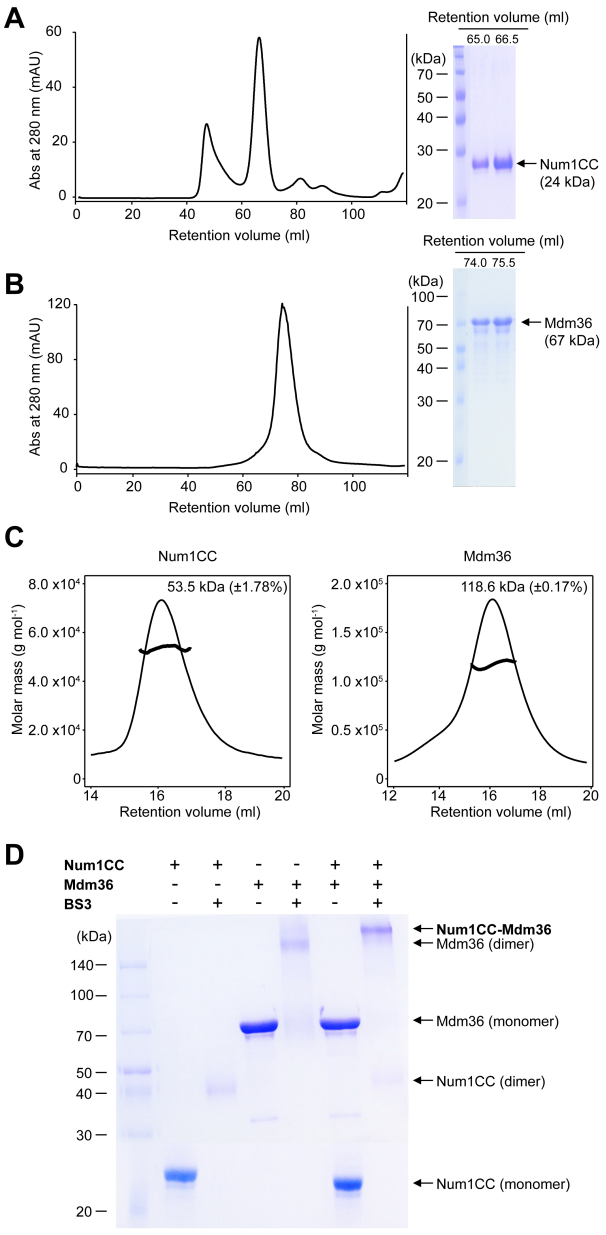

Fig. 1. Purification, SEC-MALS and chemical crosslinking of Num1CC and Mdm36. (A and B) Purification of Num1CC and Mdm36 by size-exclusion chromatography using a HiLoad 16/60 Superdex 200 prep-grade column. Abs, absorbance. (C) SEC-MALS profiles of Num1CC (left) and Mdm36 (right). The thick lines represent measured molecular masses. (D) Chemical crosslinking of Num1CC, Mdm36, and the Num1CC-Mdm36 mixture. Ten micromolar of each protein sample or mixture was mixed with BS3 at a working concentration of 500 μM and incubated at room temperature for 30 min. The reactions were quenched with 1.5 M Tris-HCl, pH 7.5.

mitochondrial fission. It should be noted that the binding affinity of the multisubunit tethering complex Dsl1 and soluble N-ethylmaleimide-sensitive factor attachment protein receptor was similar to that of the Num1CC-Mdm36 complex

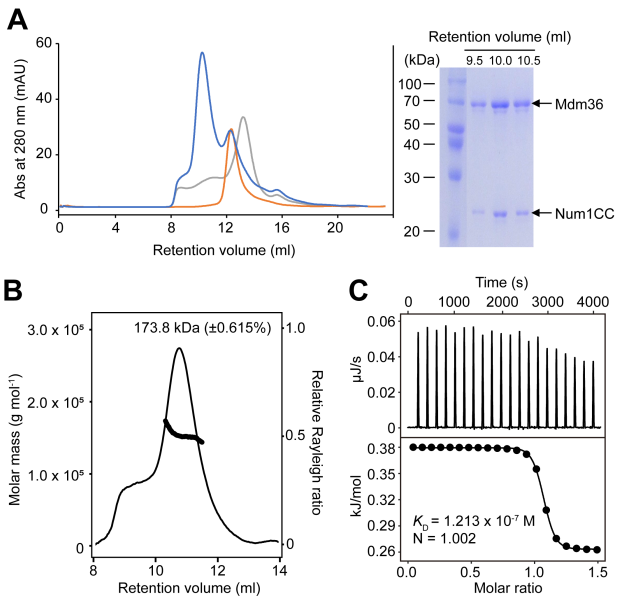

Fig. 2. Biochemical analysis of the oligomeric state, stoichiometry, and binding affinity of the Num1CC-Mdm36 complex. (A) Purification of the Num1CC-Mdm36 complex by size-exclusion chromatography using a Superdex 200 10/300 GL column. Co-elution of Num1CC and Mdm36 was observed. The blue line corresponds to the Num1CC-Mdm36 complex, while the orange line corresponds to Num1CC, and the gray line to Mdm36. Abs, absorbance. (B) Molecular weight estimation of the Num1CC-Mdm36 complex by SEC-MALS. The thick line represents measured molecular mass. The experimental molecular weight 173.8 kDa corresponds to the combination of two Num1CC and two Mdm36 molecules. (C) ITC analysis of Num1CC into Mdm36 solution. Mdm36 was titrated against Num1CC.

(Travis et al., 2020). Furthermore, the ITC experiment also indicated that the stoichiometry of Num1CC and Mdm36 was 1:1, which was consistent with the results previously anticipated by the SEC-MALS experiment (Fig. 2C).

Hydrodynamic analysis of the Num1-Mdm36 complex

Based on size-exclusion chromatography profiles of both Num1CC and Mdm36 (Fig. 1), we estimated the hydrodynamic radii of Num1CC and Mdm36. Consistent with other coiled-coil domains, Num1CC showed an unusually large hydrodynamic radius of 51.8 Å despite its relatively small dimeric molecular weight of 48 kDa. β-Amylase, which was used for the calibration of the gel-filtration column, has a molecular weight of 200 kDa and a hydrodynamic radius of 53.5 Å. Meanwhile, the hydrodynamic radius of Mdm36 was predicted as 45.7 Å, which indicates that the Mdm36 dimer (134 kDa) may exist in a globular conformation, considering that the molecular weight and hydrodynamic radius of alcohol dehydrogenase are 150 kDa and 45.4 Å, respectively.

In the case of the Num1CC-Mdm36 complex, the hydrodynamic radii of Num1CC-Mdm36 could increase by a very

small extent if globular Mdm36 interacted with the middle part of Num1CC, resulting in a globular complex. However, the predicted hydrodynamic radius of the Num1CC-Mdm36 complex was 66.8 Å, which is larger than that expected. Therefore, we postulated that Mdm36 may bind to the edge of Num1CC, thereby generating an asymmetrical complex.

Precise domain mapping of the interaction between Num1 and Mdm36

Based on the predicted hydrodynamic radii of Num1CC, Mdm36, and the Num1CC-Mdm36 complex, we reasoned that not all 198 amino acids comprising putative extended Num1CC may participate in the interaction with Mdm36. Thus, we attempted to further narrow down the binding domain of Num1CC. First, we roughly divided Num1CC (residues 97-294) to make two truncated Num1CC proteins: the N-terminal half of Num1CC (hereafter Num1 [97-195]) and the C-terminal half of Num1CC (hereafter Num1 [196-294]) (Fig. 3A). We fused GST at the N-terminus of Num1 (97-195) and Num1 (196-294), expressed both proteins in *E. coli*, and purified them by GST-affinity chromatography. Next, the GST tag was cleaved by TEV protease to prepare the dimeric forms of truncated Num1CCs. To enable complex formation, Mdm36 was added to both truncated Num1CCs, and analytical size-exclusion chromatography was performed to identify the direct interaction between Mdm36 and truncated Num1CCs. As a result, a new peak was observed with a clear peak shift in elution volume when Mdm36 was mixed with Num1 (97-195), whereas almost exact ly superimposed peaks were observed in the case of Num1 (196-294), indicating that the N-terminus of Num1CC is important for Mdm36 binding (Figs. 3B and 3C).

Next, we truncated 20 amino acids at the N- or C-terminus of Num1 (97-195) for precise mapping, thereby generating the following constructs: Num1 (117-195) and Num1 (97-175) (Fig. 3A). Then, we performed analytical size-exclusion chromatography, as described. Interestingly, Num1 (97-175), but not Num1 (117-195), bound to Mdm36, although the difference was only 20 amino acids (Figs. 3D and 3E). Considering that Mdm36 is peripherally bound to the mitochondrial surface (Hammermeister et al., 2010), it would be more favorable for Mdm36 to bind to the N-terminal part

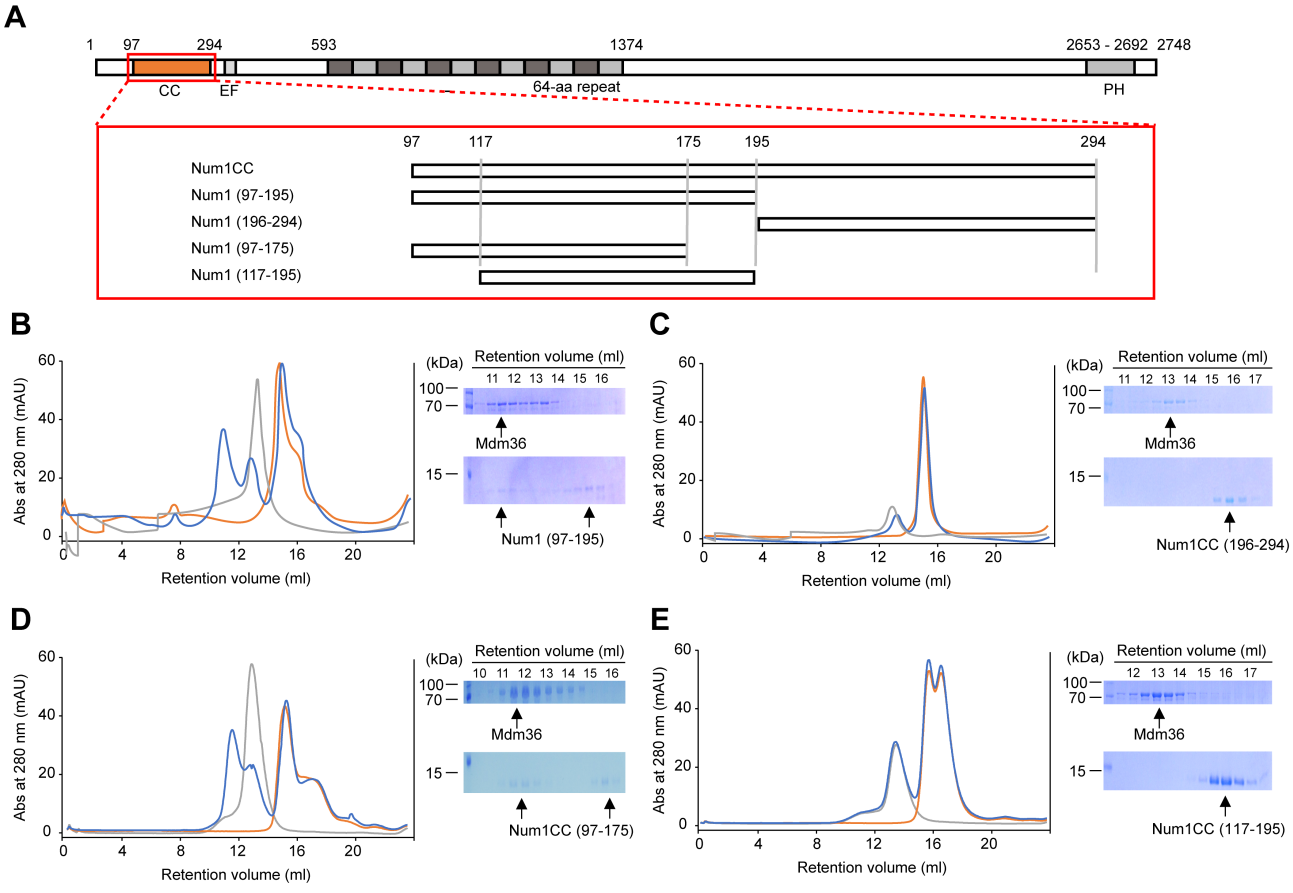

Fig. 3. Analytical size-exclusion chromatography profiles of various Num1CC-Mdm36 complexes. (A) Schematic domain architecture of Num1 (top; the coiled-coil domain is highlighted in orange in the red box), and truncated Num1CC constructs used in this study (bottom; constructs are depicted with magnification). CC, coiled-coil; EF, EF hand-like domain; PH, pleckstrin homology domain. (B-E) Analytical size-exclusion chromatograms and SDS-PAGE analyses of the complex formation between Mdm36 and truncated Num1CC proteins. Superdex 200 10/300 GL column (Cytiva) was used for analytical size-exclusion chromatography. Orange chromatograms correspond to Num1CC constructs, gray to Mdm36, and blue to various Num1CC-Mdm36 mixtures, respectively. Abs, absorbance.

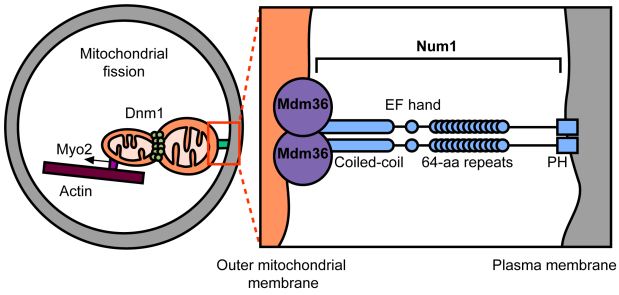

Fig. 4. Model of the Num1-Mdm36 complex in mitochondrial fission. The Num1-Mdm36 complex acts as a mitochondria-plasma membrane anchor (left). Detailed architecture of the Num1-Mdm36 complex is depicted (right).

of Num1CC rather than to the C-terminal part. In this way, Mdm36 can maintain proximity to the mitochondria by binding to the N-terminus of Num1CC, which is thought to be closer to the mitochondria.

Overall model

Based on our results, we propose a revised binding model of the Num1-Mdm36 complex at the mitochondria-plasma MCS (Fig. 4). It is known that Num1 undergoes dimerization through the coiled-coil domain, although it cannot be ruled out that other domains may contribute to the dimerization of Num1 (Tang et al., 2012). Num1 has two domains at the N- and C-termini: the coiled-coil domain and the PH domain. Both domains have different lipid binding specificities (Ping et al., 2016), and the cardiolipin-specific coiled-coil domain interacts with mitochondria, whereas the $PI_{4,5}P_2$-specific PH domain interacts with the plasma membrane. Thus, it is likely that the overall length of Num1 might be close to that of the intermembrane gap of the mitochondria and plasma membrane. Mdm36 also exists as a dimer, and it interacts preferentially with the N-terminal half of Num1CC with a stoichiometry of 2:2, forming a heterotetramer. In particular, the first 20 amino acids in Num1CC were important for binding in our experiment. Considering that dimeric Num1 stretches between the mitochondria and plasma membrane, dimeric Mdm36 binds to the proximal mitochondrial membrane, as well as to the N-terminal edge of Num1CC. Taken together, although additional structural studies are needed to fully understand the molecular architecture of the Num1-Mdm36 complex, we expect that our biochemical characterization and stoichiometric model of the Num1-Mdm36 complex can serve as a foundation for further investigation to understand the molecular mechanism of mitochondria-plasma membrane tethering in budding yeast.

ACKNOWLEDGMENTS

This study was also supported by a grant from the National Research Foundation (NRF) of Korea, funded by the Korean government (2015R1A5A1008958, 2015M3D3A1A01064919, and 2018R1A2B2008142).

AUTHOR CONTRIBUTIONS

J.W. and H.H.L. conceived the experiments and wrote the manuscript. J.W., Y.C., and Y.Y. performed the experiments, and H.H.L. directed the team and secured funding.

CONFLICT OF INTEREST

The authors have no potential conflicts of interest to disclose.

ORCID

Jongdae Won https://orcid.org/0000-0003-2946-0791
Yuri Choi https://orcid.org/0000-0002-9188-3747
Yaejin Yun https://orcid.org/0000-0003-2721-3789
Hyung Ho Lee https://orcid.org/0000-0003-1168-2484

REFERENCES

Booth, D.M., Enyedi, B., Geiszt, M., Várnai, P., and Hajnóczky, G. (2016). Redox nanodomains are induced by and control calcium signaling at the ER-mitochondrial interface. Mol. Cell *63*, 240-248.

Cerveny, K.L., Studer, S.L., Jensen, R.E., and Sesaki, H. (2007). Yeast mitochondrial division and distribution require the cortical num1 protein. Dev. Cell *12*, 363-375.

Chen, W., Ping, H.A., and Lackner, L.L. (2018). Direct membrane binding and self-interaction contribute to Mmr1 function in mitochondrial inheritance. Mol. Biol. Cell *29*, 2346-2357.

de Brito, O.M. and Scorrano, L. (2008). Mitofusin 2 tethers endoplasmic reticulum to mitochondria. Nature *456*, 605-610.

Dong, D., Huang, X., Li, L., Mao, H., Mo, Y., Zhang, G., Zhang, Z., Shen, J., Liu, W., Wu, Z., et al. (2020). Super-resolution fluorescence-assisted diffraction computational tomography reveals the three-dimensional landscape of the cellular organelle interactome. Light Sci. Appl. *9*, 11.

Eisenberg-Bord, M., Shai, N., Schuldiner, M., and Bohnert, M. (2016). A tether is a tether is a tether: tethering at membrane contact sites. Dev. Cell *39*, 395-409.

García De La Torre, J., Huertas, M.L., and Carrasco, B. (2000). Calculation of hydrodynamic properties of globular proteins from their atomic-level structure. Biophys. J. *78*, 719-730.

Hammermeister, M., Schodel, K., and Westermann, B. (2010). Mdm36 is a mitochondrial fission-promoting protein in Saccharomyces cerevisiae. Mol. Biol. Cell *21*, 2443-2452.

Hayashi, T., Rizzuto, R., Hajnoczky, G., and Su, T.P. (2009). MAM: more than just a housekeeper. Trends Cell Biol. *19*, 81-88.

Helle, S.C., Kanfer, G., Kolar, K., Lang, A., Michel, A.H., and Kornmann, B. (2013). Organization and function of membrane contact sites. Biochim. Biophys. Acta *1833*, 2526-2541.

Huang, X., Jiang, C., Yu, L., and Yang, A. (2020). Current and emerging approaches for studying inter-organelle membrane contact sites. Front. Cell Dev. Biol. *8*, 195.

Kakimoto, Y., Tashiro, S., Kojima, R., Morozumi, Y., Endo, T., and Tamura, Y. (2018). Visualizing multiple inter-organelle contact sites using the organelle-targeted split-GFP system. Sci. Rep. *8*, 6175.

Kormanec, J., Schaaff-Gerstenschläger, I., Zimmermann, F.K., Perecko, D., and Küntzel, H. (1991). Nuclear migration in Saccharomyces cerevisiae is controlled by the highly repetitive 313 kDa NUM1 protein. Mol. Gen. Genet. *230*, 277-287.

Kraft, L.M. and Lackner, L.L. (2018). Mitochondrial anchors: positioning mitochondria and more. Biochem. Biophys. Res. Commun. *500*, 2-8.

Lackner, L.L., Ping, H., Graef, M., Murley, A., and Nunnari, J. (2013). Endoplasmic reticulum-associated mitochondria-cortex tether functions in the distribution and inheritance of mitochondria. Proc. Natl. Acad. Sci. U. S. A. *110*, E458-E467.

Naon, D. and Scorrano, L. (2014). At the right distance: ER-mitochondria

juxtaposition in cell life and death. Biochim. Biophys. Acta *1843*, 2184-2194.

Nascimbeni, A.C., Giordano, F., Dupont, N., Grasso, D., Vaccaro, M.I., Codogno, P., and Morel, E. (2017). ER-plasma membrane contact sites contribute to autophagosome biogenesis by regulation of local PI3P synthesis. EMBO J. *36*, 2018-2033.

Ouasti, S., Matarrese, P., Paddon, R., Khosravi-Far, R., Sorice, M., Tinari, A., Malorni, W., and Degli Esposti, M. (2007). Death receptor ligation triggers membrane scrambling between Golgi and mitochondria. Cell Death Differ. *14*, 453-461.

Ping, H.A., Kraft, L.M., Chen, W., Nilles, A.E., and Lackner, L.L. (2016). Num1 anchors mitochondria to the plasma membrane via two domains with different lipid binding specificities. J. Cell Biol. *213*, 513-524.

Prinz, W.A., Toulmay, A., and Balla, T. (2020). The functional universe of membrane contact sites. Nat. Rev. Mol. Cell Biol. *21*, 7-24.

Rizzuto, R., Pinton, P., Carrington, W., Fay, F.S., Fogarty, K.E., Lifshitz, L.M., Tuft, R.A., and Pozzan, T. (1998). Close contacts with the endoplasmic reticulum as determinants of mitochondrial Ca2+ responses. Science *280*, 1763-1766.

Shai, N., Yifrach, E., van Roermund, C.W.T., Cohen, N., Bibi, C., IJlst, L., Cavellini, L., Meurisse, J., Schuster, R., Zada, L., et al. (2018). Systematic mapping of contact sites reveals tethers and a function for the peroxisome-mitochondria contact. Nat. Commun. *9*, 1761.

Tang, X., Germain, B.S., and Lee, W.L. (2012). A novel patch assembly domain in Num1 mediates dynein anchoring at the cortex during spindle positioning. J. Cell Biol. *196*, 743-756.

Travis, S.M., DAmico, K., Yu, I.M., McMahon, C., Hamid, S., Ramirez-Arellano, G., Jeffrey, P.D., and Hughson, F.M. (2020). Structural basis for the binding of SNAREs to the multisubunit tethering complex Dsl1. J. Biol. Chem. *295*, 10125-10135.

Valm, A.M., Cohen, S., Legant, W.R., Melunis, J., Hershberg, U., Wait, E., Cohen, A.R., Davidson, M.W., Betzig, E., and Lippincott-Schwartz, J. (2017). Applying systems-level spectral imaging and analysis to reveal the organelle interactome. Nature *546*, 162-167.

Westermann, B. (2015). The mitochondria-plasma membrane contact site. Curr. Opin. Cell Biol. *35*, 1-6.